Electronic Supplementary Material (ESI) for ChemComm.

Supporting Information

Chiroptical Switching Caused by Crystalline/Liquid Crystalline Phase Transition of a Chiral Bowl-shaped Molecule

Masaki Yamamura,* Kimiya Sukegawa, Daichi Okada, Yohei Yamamoto, Tatsuya Nabeshima*

Graduate School of Pure and Applied Sciences, Tsukuba Research Center for Interdisciplinary Materials Science (TIMS), University of Tsukuba
1-1-1, Tennodai, Tsukuba, Ibaraki 305-8571, Japan

E-mail: myama@chem.tsukuba.ac.jp, nabesima@chem.tsukuba.ac.jp,

Table of contents

(1) General methods

All chemicals were reagent grade, and used without further purification. All reactions were performed under a nitrogen atmosphere. Chromatography was performed using SiO_2-60N (0.063–0.212 mm; Kanto). The ^{1}H and ^{13}C NMR spectra were recorded on Bruker AVANCE400 (400 MHz) spectrometer using tetramethylsilane (0 ppm) and $CDCl_3$ (77 ppm) as internal standards. The ^{31}P NMR spectra were recorded on Bruker AVANCE400 (400 MHz) spectrometer using phosphoric acid (0 ppm) as an external standard. Deuterated solvents were purchased from Cambridge Isotope Laboratories or Aldrich and used as received. MALDI-TOF mass spectra were recorded on an AB Sciex TOF/TOF5800. Elemental analysis was performed at Department of Chemistry, University of Tsukuba. X-ray diffraction (XRD) patterns were recorded on a Rigaku model Miniflex600 X-ray diffractometer with a Cu Kα radiation source. Small-angle X-ray scattering (SAXS) patterns were recorded on a Rigaku MicroMax-007HF with a Cu Kα radiation source. Differential scanning calorimetry (DSC) was measured on a SEIKO Instruments model EXSTART7000 differential scanning calorimeter using Al pan under Ar atmosphere at the scan rate of 10 ºC/min. UV-vis absorption spectra were recorded on a JASCO V-670. Circular dichroism (CD) spectra were recorded on a JASCO J-820. Atomic Force Microscopy (AFM) was performed on a SII NanoTechnology S-image unit with a NanoNavi Station working on tapping mode with a silicon cantilever at a working frequency of 126 kHz.

(2) Synthetic procedure

Compound **3** was synthesized from tribromophosphangulene **5**[S1] and 3,4,5-tridodecyloxyphenyl-acetylene **6**.[S2] Compounds **5** and **6** were prepared according to literatures.

Synthesis of 3

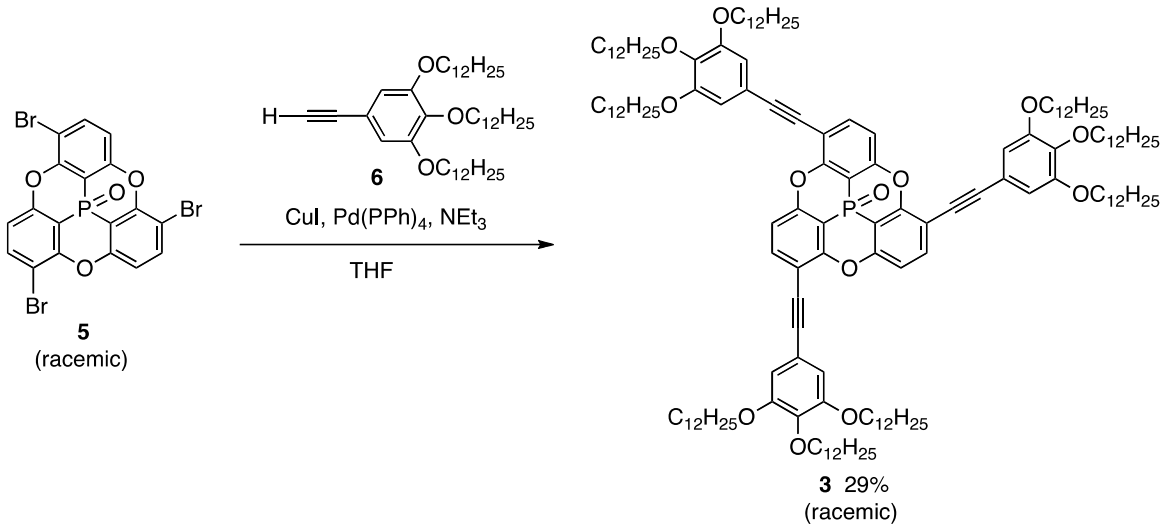

To a THF solution (14 mL) of racemic tribromophosphangulene **5** (104.2 mg, 187 μmol), CuI (4 mg, 21 μmol), $Pd(PPh_3)_4$ (25 mg, 22 μmol), and **6** (430 mg, 656 μmol) was added degassed NEt_3 (8 mL) and the mixture was stirred at 70 ºC for 17 hours. After the removal of the solvent under vacuum, the crude product was separated by silica-gel column chromatography (eluent: chloroform) to give a pale-brown viscos paste of *rac*-**3** (124.9 mg, 29%). The racemic mixture was separated to enantiomers by DAICEL CHIRALPAK IA (eluent: chloroform/hexane = 1/1).

rac-**3**: ^{1}H NMR (400 MHz, $CDCl_3$) δ 0.84-0.90 (m, 27H), 1.20-1.54 (m, 162H), 1.72-1.87 (m, 18H), 3.97-4.04 (m, 18H), 6.80 (s, 6H), 7.29 (dd, J = 8.4 Hz, 4.8 Hz, 3H), 7.67 (d, J = 8.4 Hz, 3H); ^{13}C NMR (101 MHz, $CDCl_3$) δ 14.1, 22.7, 26.1, 29.4, 29.4, 29.4, 29.6, 29.7, 29.7, 29.8, 29.8, 30.3, 31.9, 32.0, 69.3, 73.6, 80.9, 96.1, 109.7 (d, $J_{C\text{-}P}$ = 100.7Hz), 110.4, 111.7 (d, $J_{C\text{-}P}$ = 6.4 Hz), 115.7, 117.0, 137.0, 139.8, 153.1, 158.8, 157.8; ^{31}P NMR (162 MHz, $CDCl_3$) δ –50.0; MALDI-TOFMS *m/z* 2280.11 $[M+H]^+$; Anal. Calcd for $C_{150}H_{237}O_{13}P$: C, 79.04; H, 10.48. Found: C, 78.97; H, 10.45.

Synthesis of 4

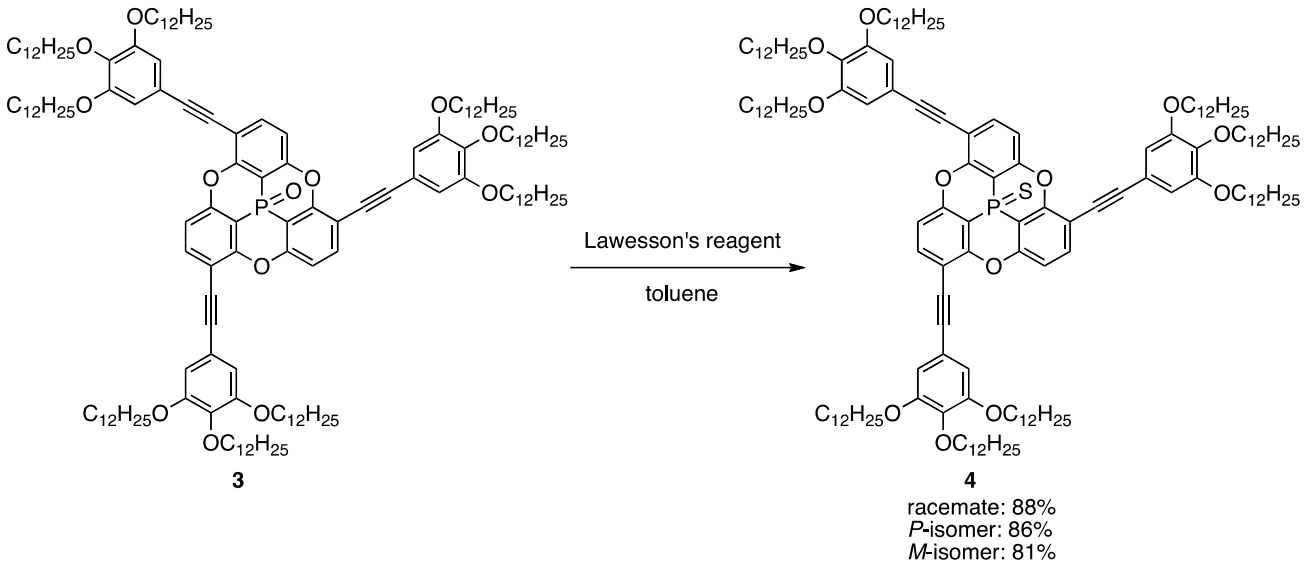

A toluene (4 mL) solution of *rac*-**4** (38.3 mg, 16.8 μmol) and Lawesson's reagent (9.6 mg, 237 μmol) was refluxed for 16 hours. After the removal of the solvent under vacuum, the crude product was separated by silica-gel column chromatography (eluent: chloroform/hexane 1/1 to 2/1) to give a pale-yellow viscos paste of *rac*-**4** (33.6 mg, 88%). *P*- and *M*-**4** were prepared from *P*- and *M*-**3** in 86 and 81% yields, respectively.

rac-**4**: ^{1}H NMR (400 MHz, $CDCl_3$) δ 0.85-0.90 (m, 27H), 1.20-1.50 (m, 162H), 1.73-1.86 (m, 18H), 3.98-4.04 (m, 18H), 6.80 (s, 6H), 7.28 (dd, J = 4.4, 8.8 Hz, 3 H), 7.62 (d, J = 8.8 Hz, 3H); ^{13}C NMR (101 MHz, $CDCl_3$) δ 14.1, 22.7, 26.1, 29.4, 29.4, 29.4, 29.6, 29.7, 29.7, 29.8, 29.8, 30.3, 31.9, 32.0, 69.3, 73.7, 81.0, 96.1, 109.8 (d, $J_{C\text{-}P}$ = 85.7 Hz), 110.4, 112.0 (d, $J_{C\text{-}P}$ = 7.1 Hz), 115.9 (d, $J_{C\text{-}P}$ = 5.3 Hz), 117.0, 136.0, 139.7, 153.1, 157.7, 157.9; ^{31}P NMR (162 MHz, $CDCl_3$) δ –53.0; MALDI-TOFMS *m/z* 2296.03 $[M+H]^+$; Anal. Calcd for $C_{150}H_{237}O_{12}PS$: C, 78.48; H, 10.41. Found: C, 78.40; H, 10.29.

Synthesis of 2

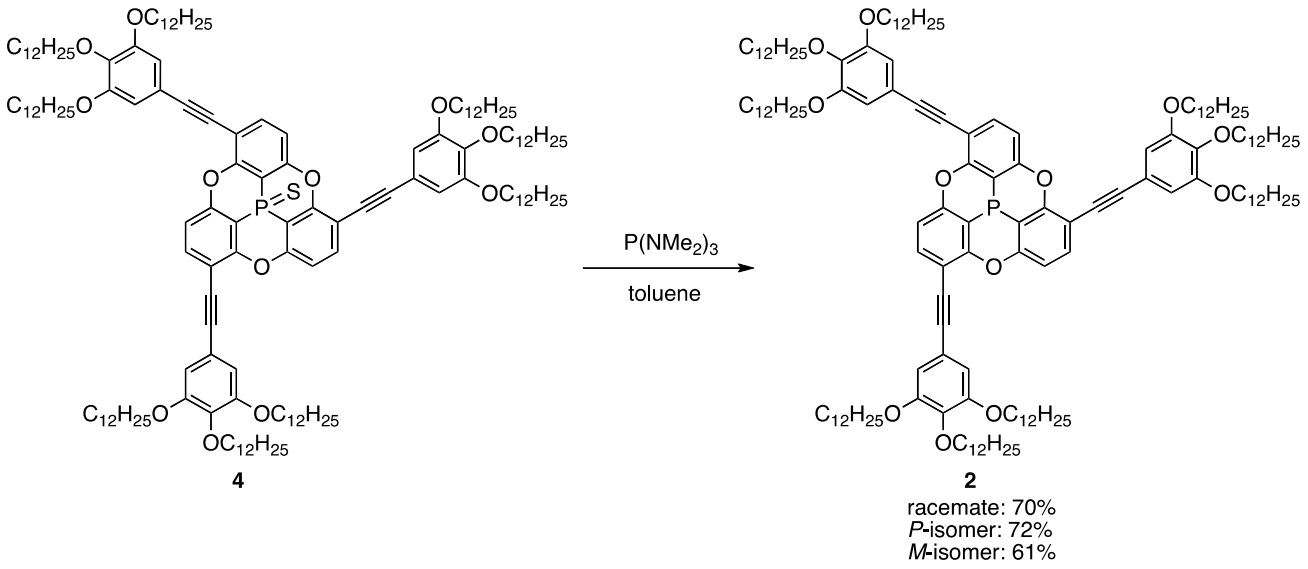

4 2

A toluene (4 mL) solution of *rac*-**4** (31.4 mg, 13.6 μmol) and $P(NMe_2)_3$ (15 μL, 237 μmol) was refluxed for 15 hours. After the removal of the solvent under vacuum, the crude product was separated by silica-gel column chromatography (eluent: chloroform/hexane 1/2) to give a colorless viscos paste of *rac*-**2** (21.6 mg, 70%). *P*- and *M*-**2** were prepared from *P*- and *M*-**4** in 72 and 61% yields, respectively.

rac-**2**: ^{1}H NMR (400 MHz, $CDCl_3$) δ 0.85-0.90 □m, 27H), 1.21-1.53 (m, 162H), 1.73-1.85 (m, 18H), 3.97-4.03 (m, 18H), 6.79 (s, 6H), 7.13 (dd, J = 8.4, 1.6 Hz, 3H), 7.46 (dd, J = 8.4, 1.6 Hz, 3H); ^{13}C NMR (101 MHz, $CDCl_3$) δ 14.1, 22.7, 26.1, 29.4, 29.4, 29.4, 29.6, 29.7, 29.7, 29.7, 29.8, 30.3, 31.9, 32.0, 69.3, 73.6, 82.0, 94.9, 109.4, 110.4, 111.4 (d, $J_{C\text{-}P}$ = 1.4 Hz), 113.7, 113.9, 115.3, 117.5, 133.5, 139.5, 153.1, 155.2 (d, $J_{C\text{-}P}$ = 7.8 Hz), 155.3 (d, $J_{C\text{-}P}$ = 7.8 Hz); ^{31}P NMR (162 MHz, $CDCl_3$) δ –132.4; MALDI-TOFMS *m/z* 2262.94 $[M]^{\bullet+}$; Anal. Calcd for $C_{150}H_{237}O_{12}P\cdot H_2O$: C, 78.97; H, 10.56. Found: C, 78.66; H, 10.69.

(3) MALDI-TOF MS of 1

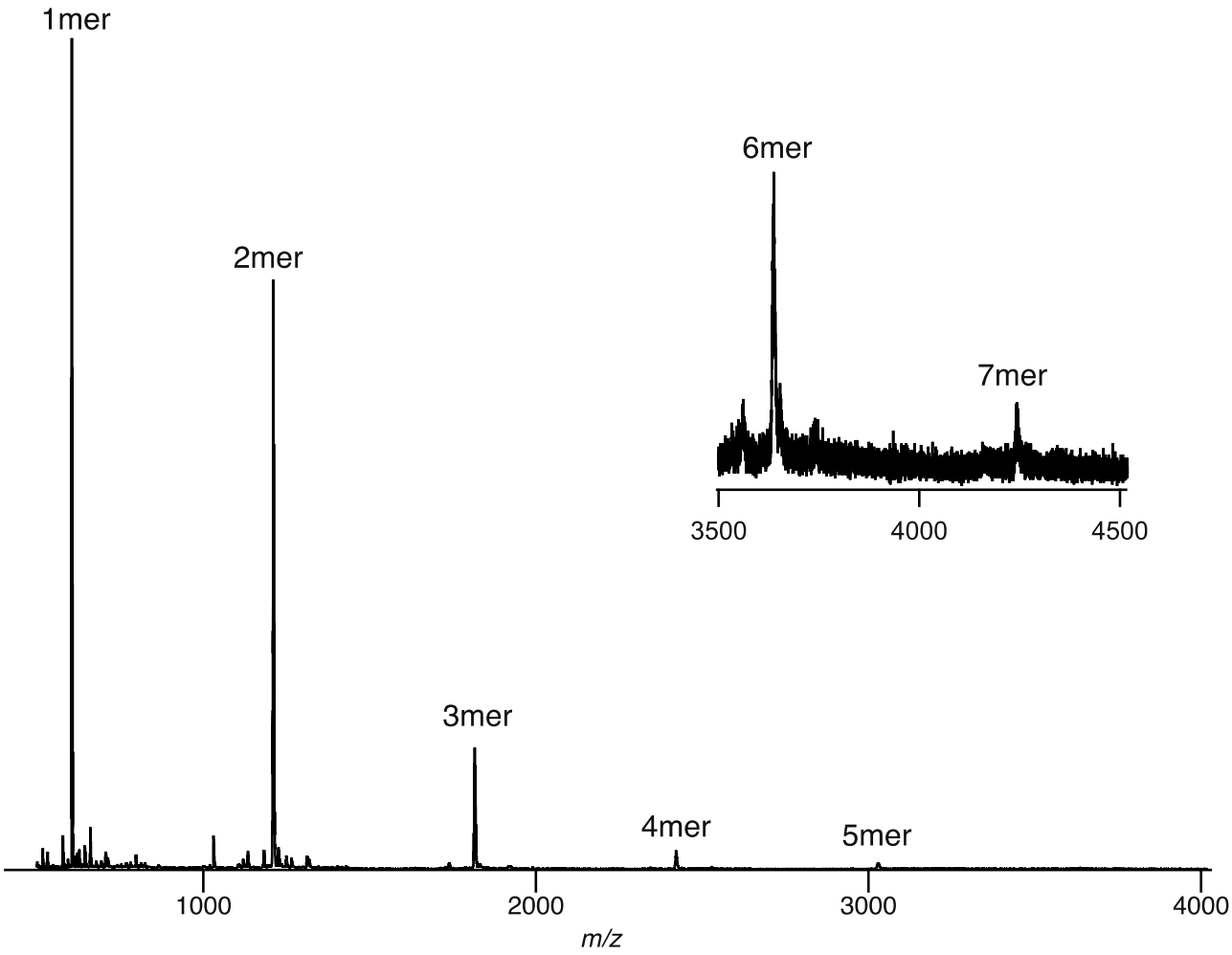

Figure S1. MALDI-TOF MS of racemic *rac*-**1**.

(4) POM

a)

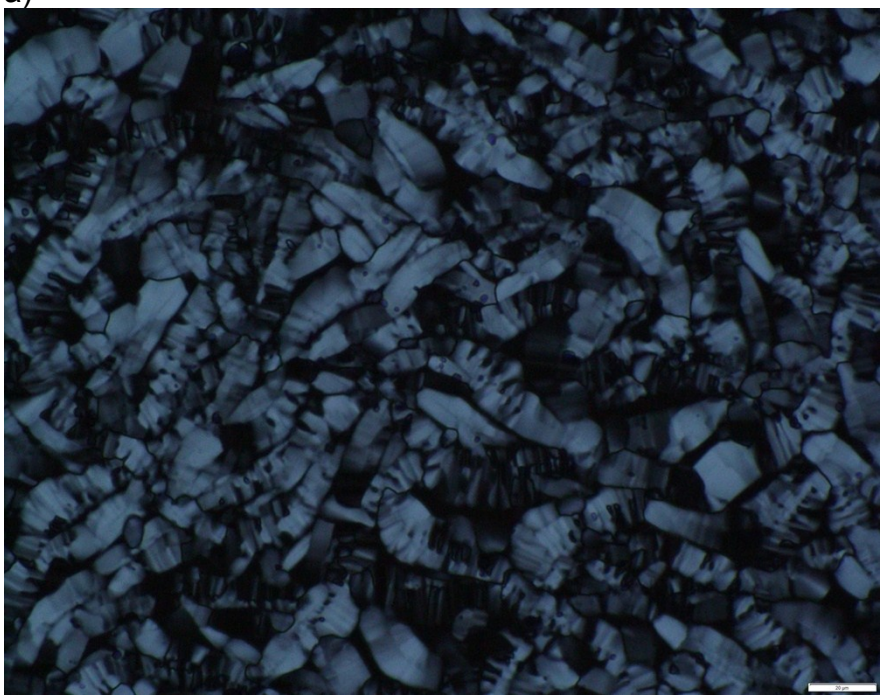

b)

Figure S2. POM of enantiopure *P*-**2** at (a) 90 ºC (liquid-crystalline phase) and (b) 120 ºC (isotropic phase).

(5) Molecular modeling

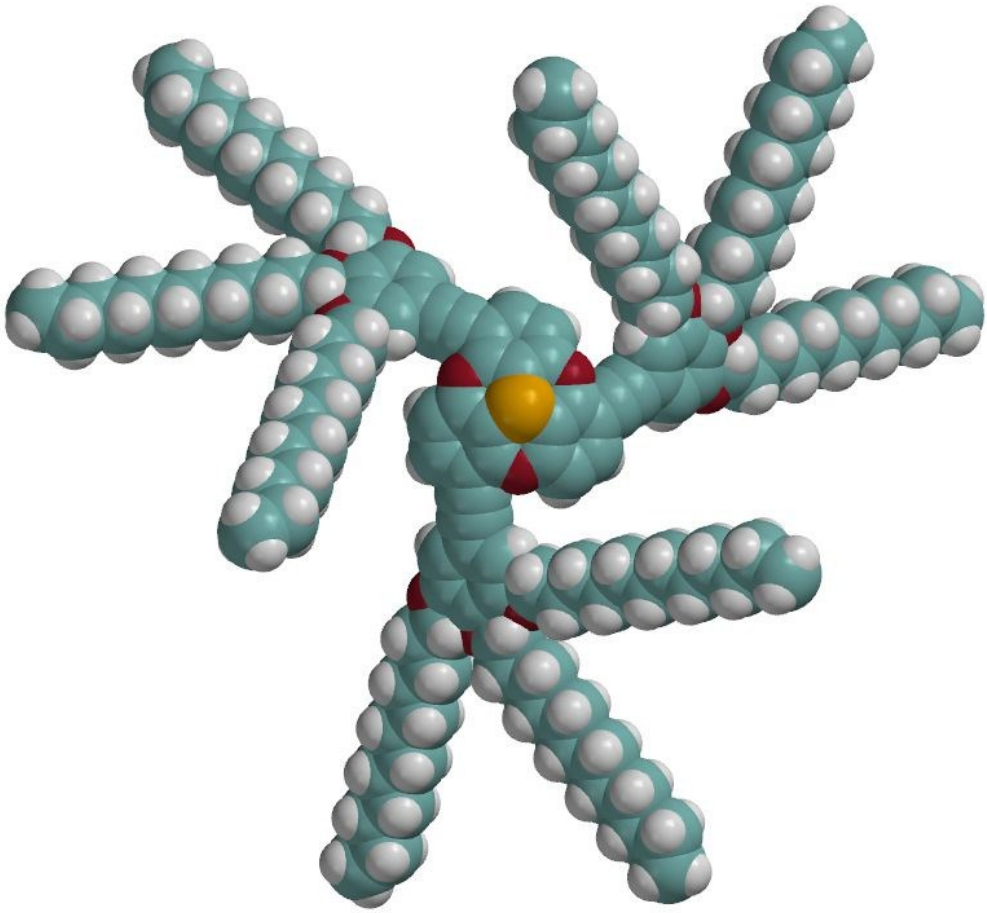

Figure S3. Molecular modeling of *M*-**2** optimized at the PM3 level of theory.

(6) SAXS

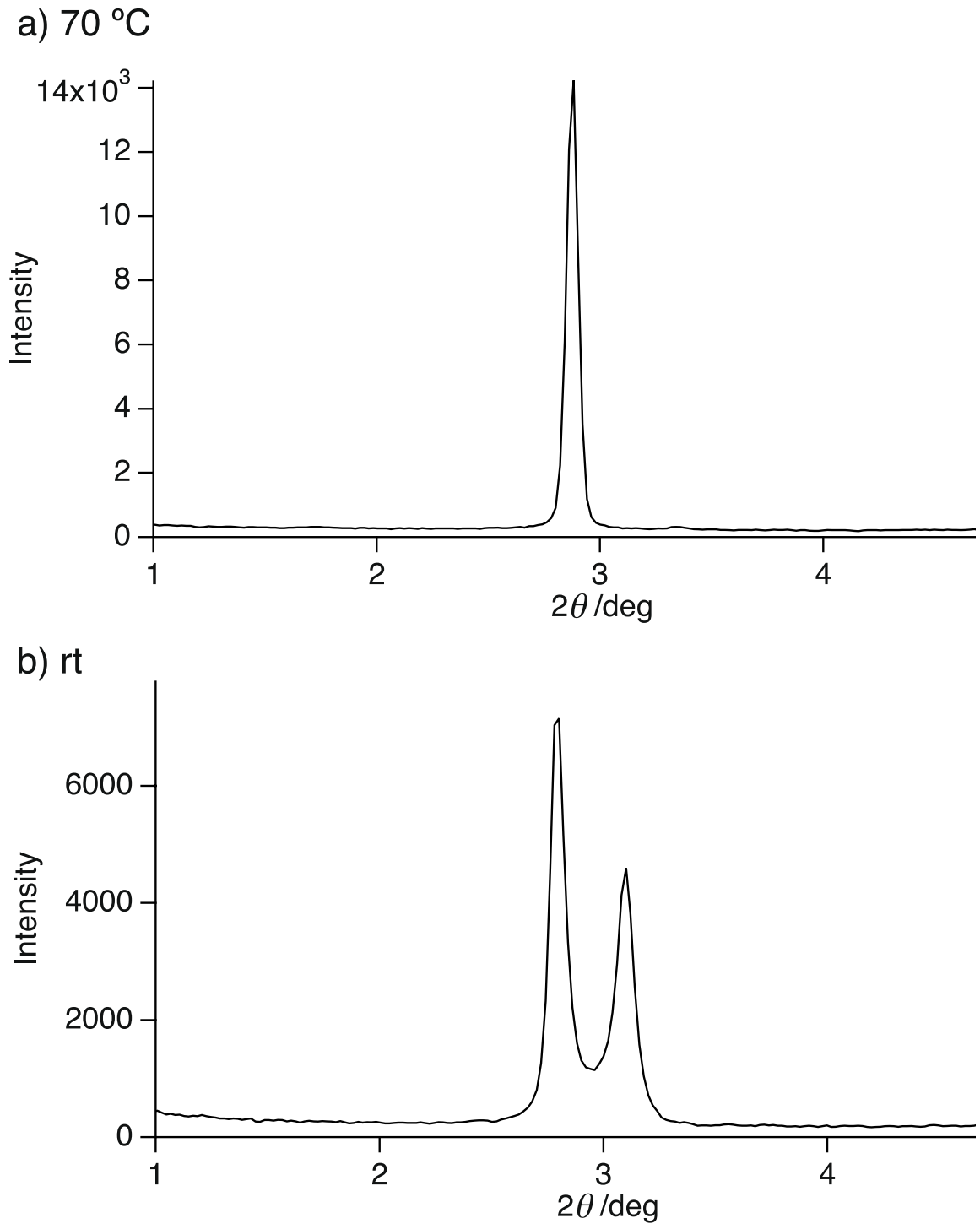

Figure S4. SAXS of enantiopure *P*-**2** at (a) 70 ºC and (b) rt.

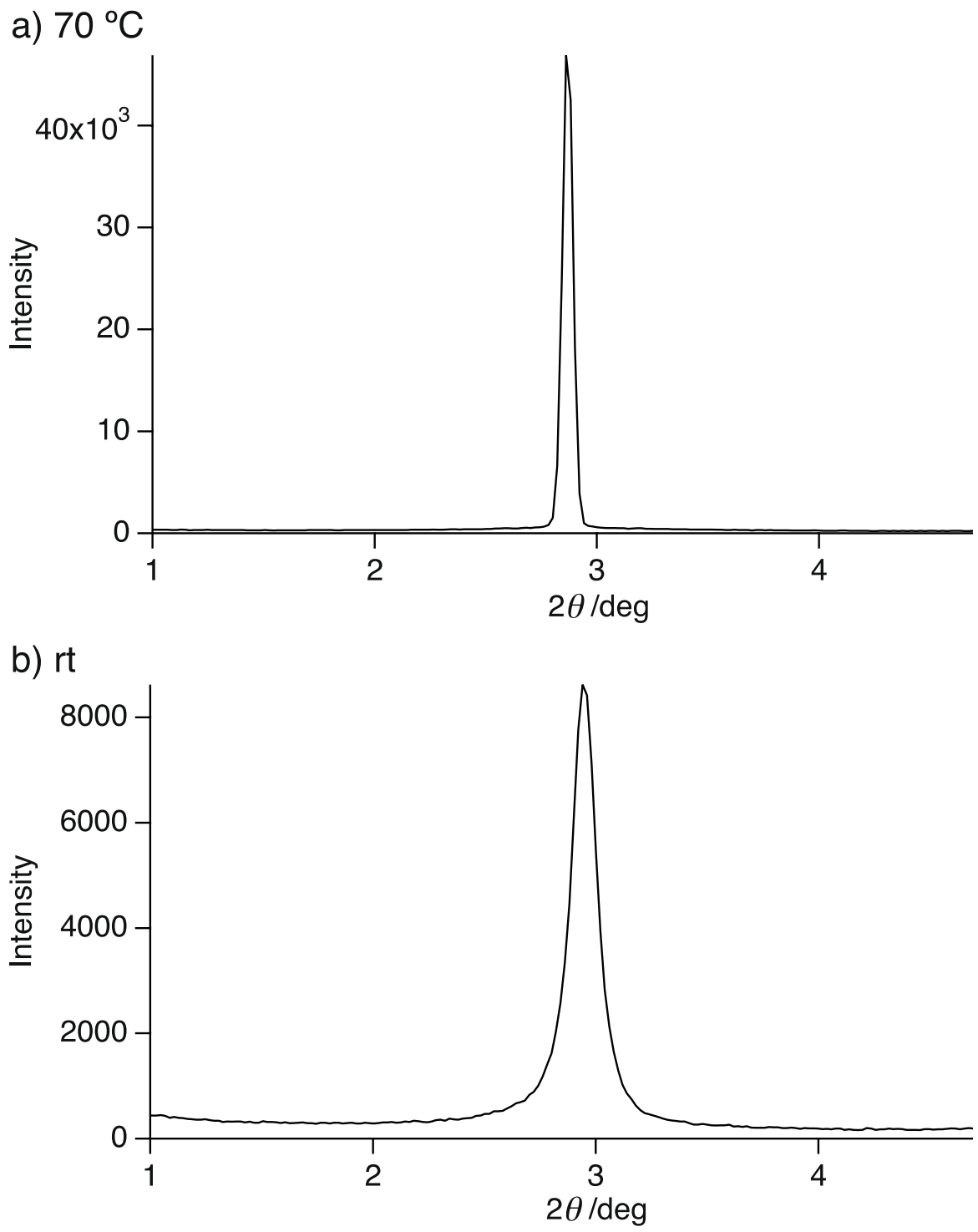

Figure S5. SAXS of *rac*-**2** at (a) 70 ºC and (b) rt.

(7) UV-vis absorption and CD spectra

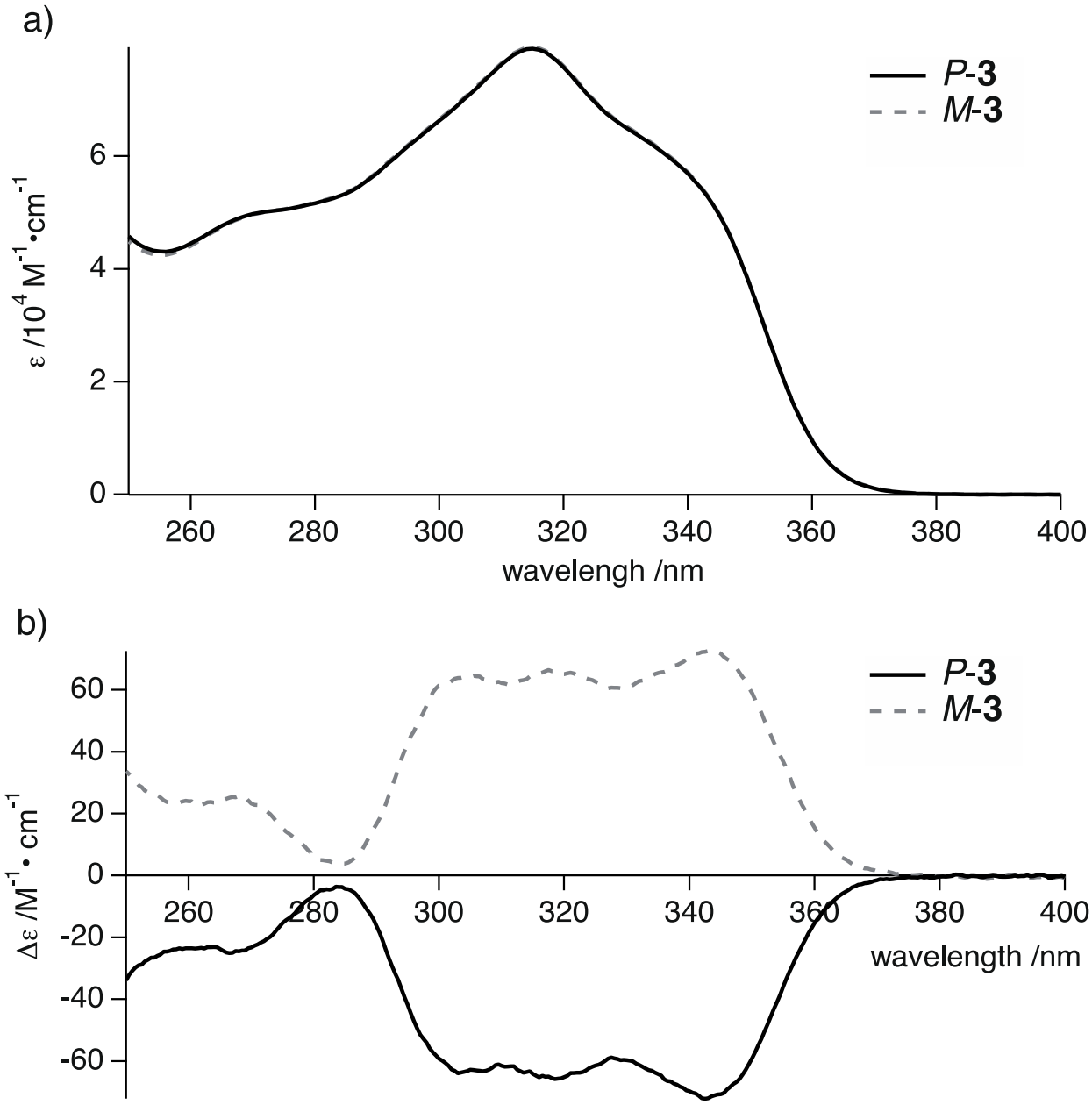

Figure S6. (a) Absorption and (b) CD spectra of *P*-**3** and *M*-**3** in chloroform.

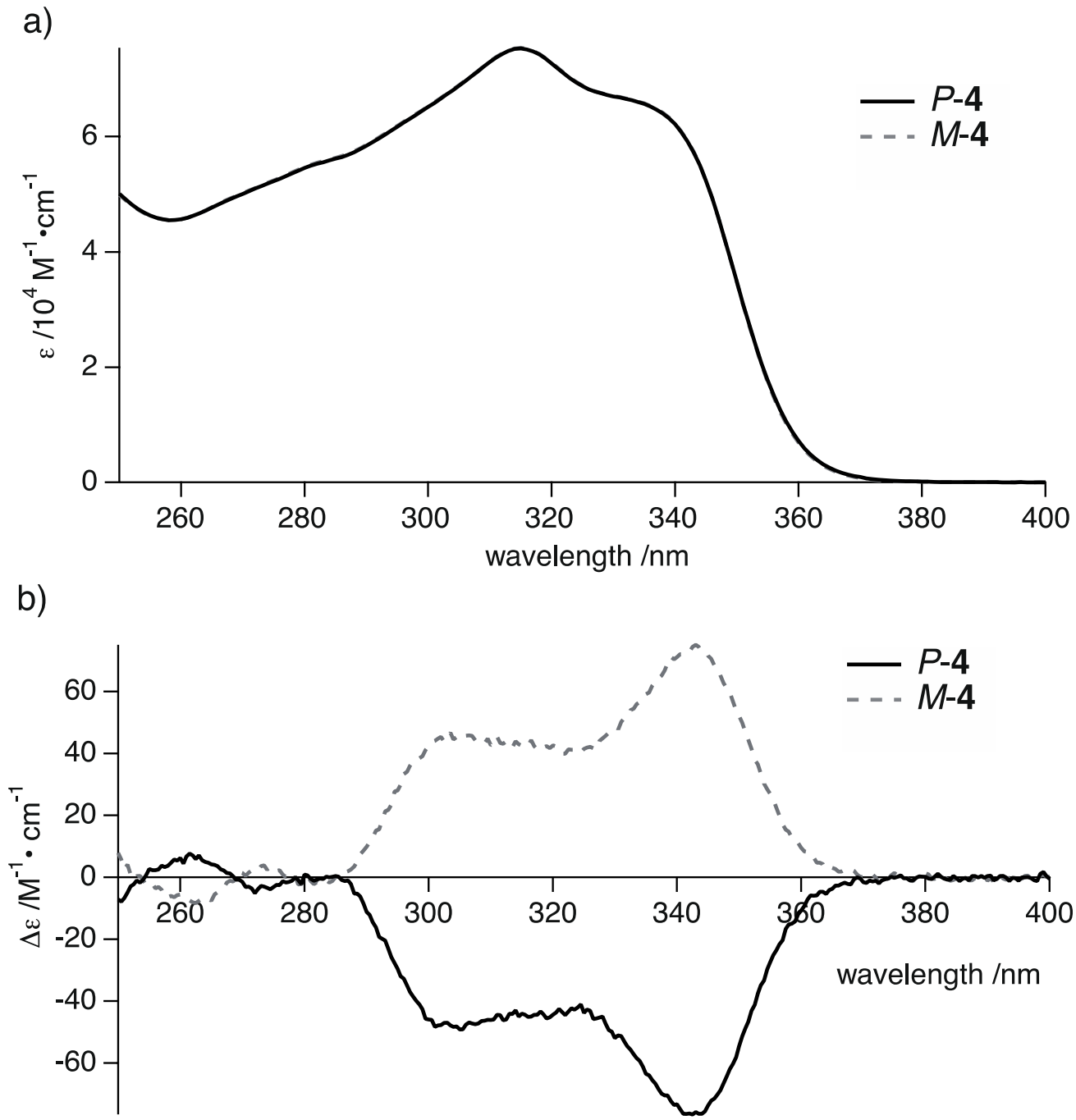

Figure S7. (a) Absorption and (b) CD spectra of *P*-**4** and *M*-**4** in chloroform.

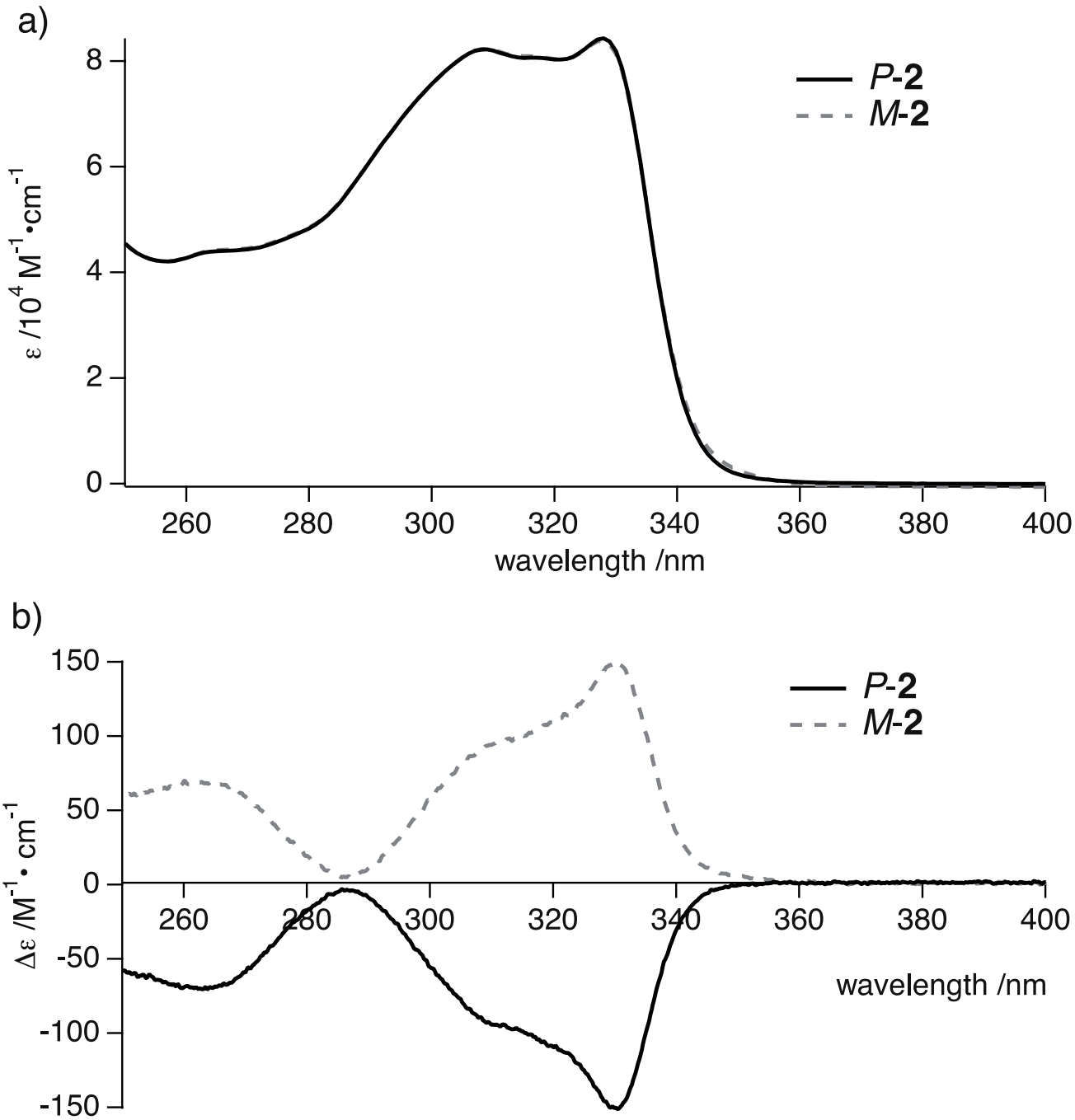

Figure S8. (a) Absorption and (b) CD spectra of *P*-**2** and *M*-**2** in cyclohexane.

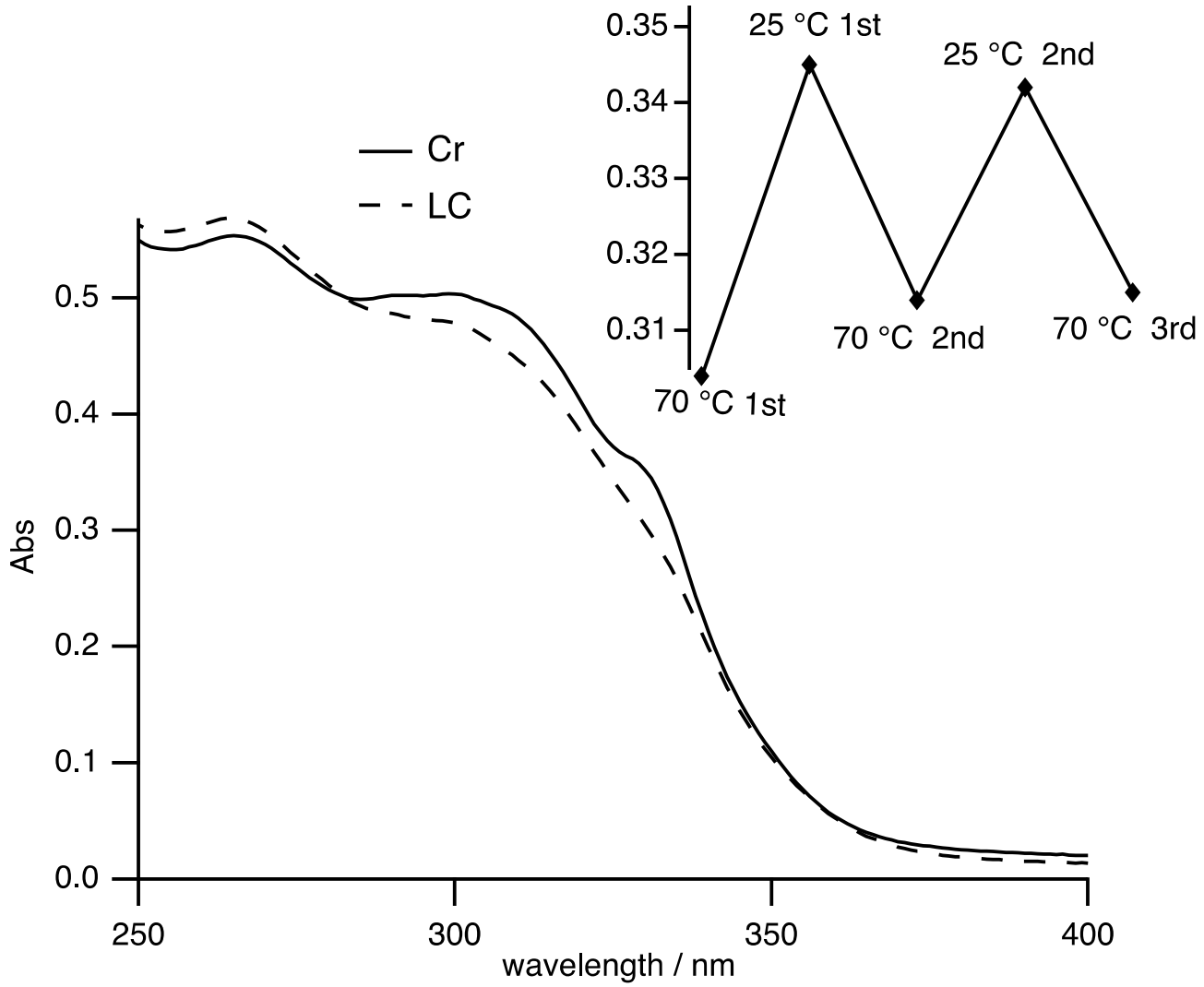

Figure S9. UV-vis absorption spectra of *P*-**2** in Cr and LC phases. Inset shows chiroptical switching at 320 nm between Cr phase (25 ºC) and LC phase (70 ºC).

(8) NMR spectra

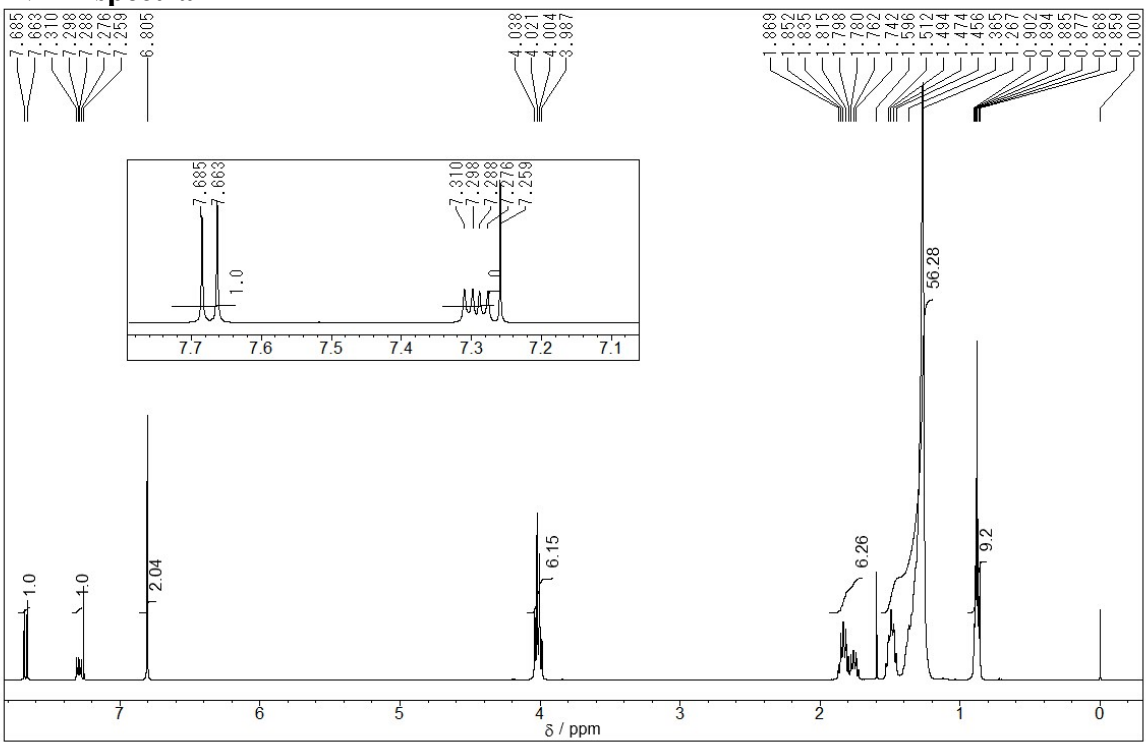

Figure S10. ^{1}H NMR spectrum of **3** (400 MHz, $CDCl_3$)

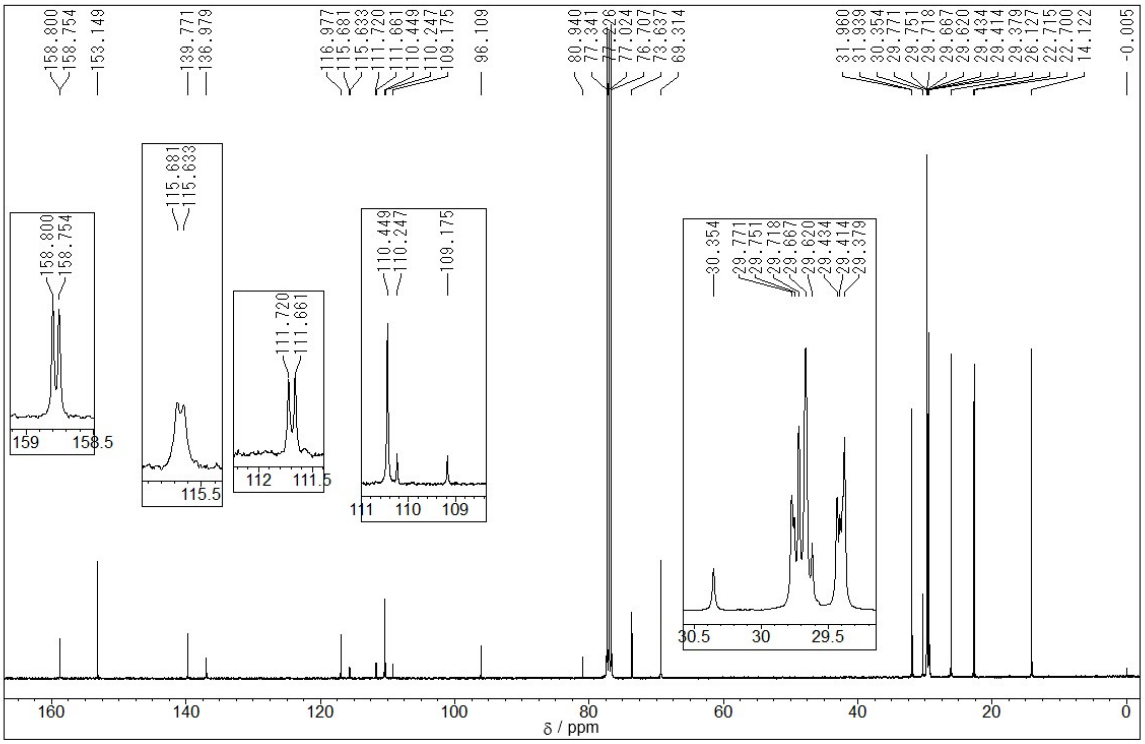

Figure S11. ^{13}C NMR spectrum of **3** (100 MHz, $CDCl_3$)

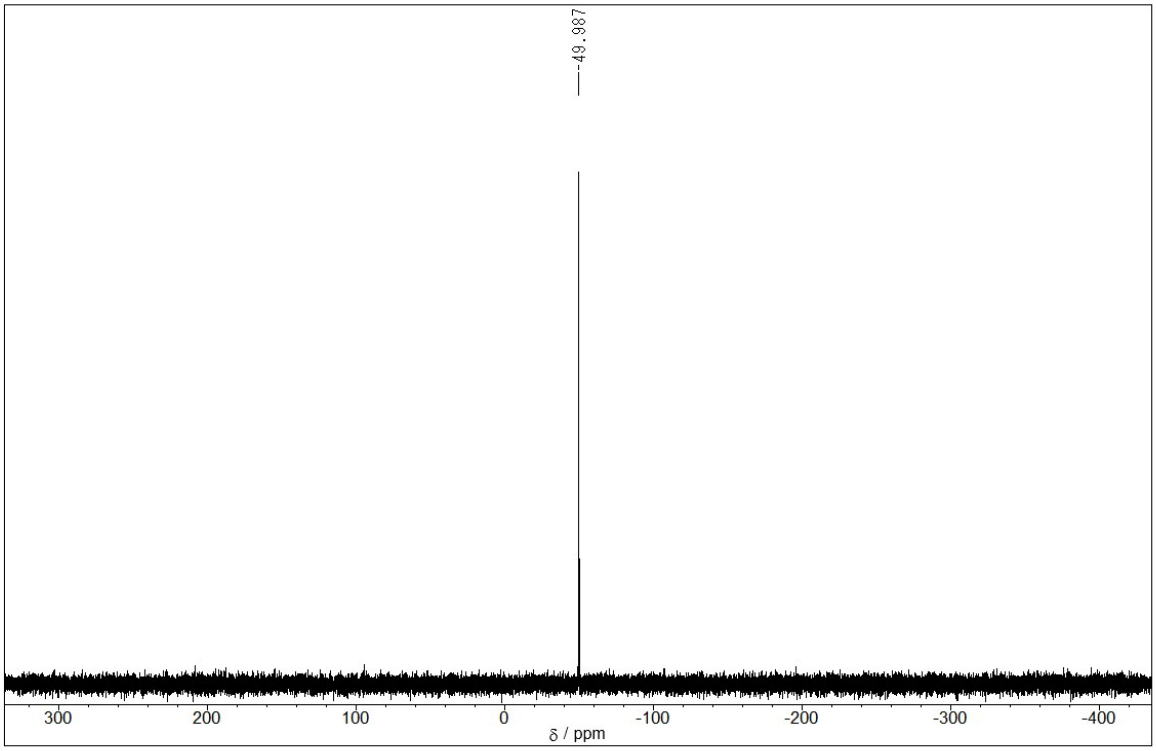

Figure S12. ^{31}P NMR spectrum of **3** (162 MHz, $CDCl_3$)

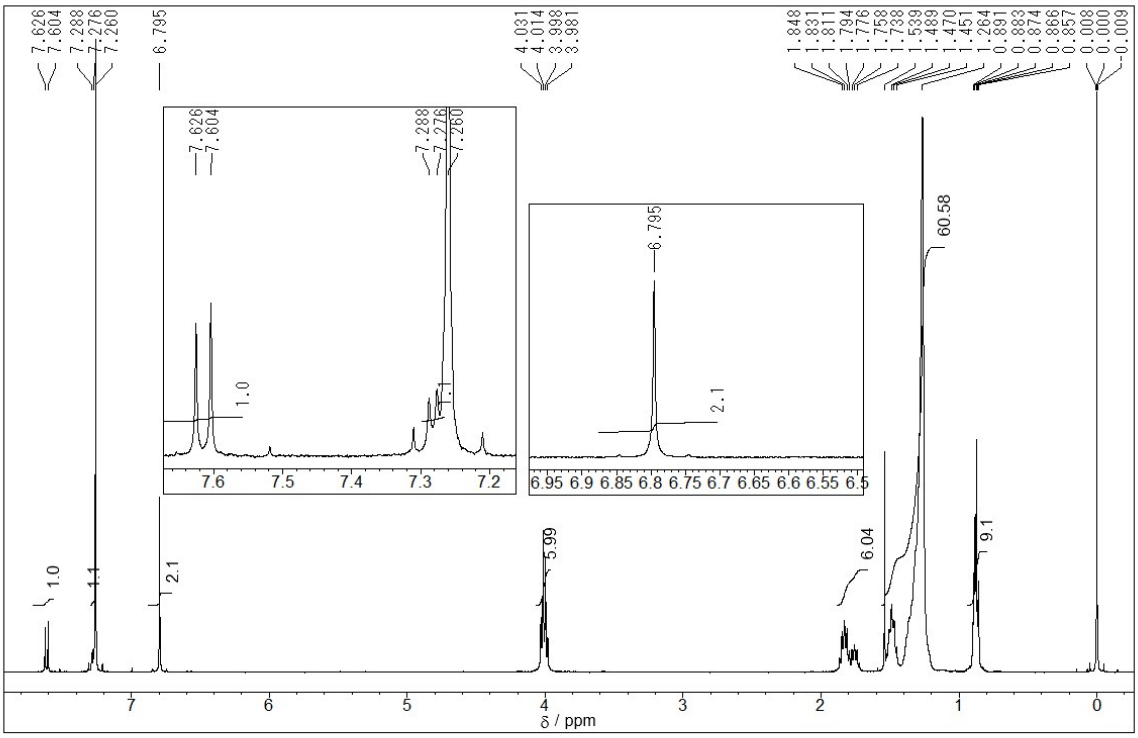

Figure S13. ^{1}H NMR spectrum of **4** (400 MHz, $CDCl_3$)

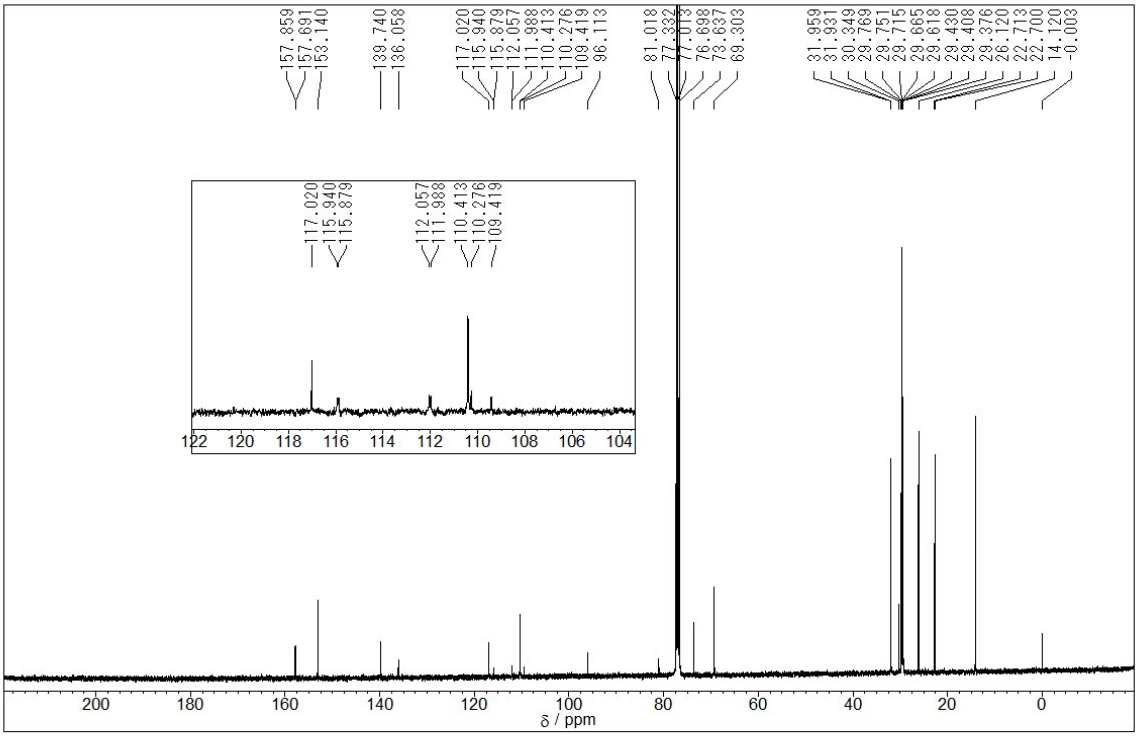

Figure S14. ^{13}C NMR spectrum of **4** (100 MHz, $CDCl_3$)

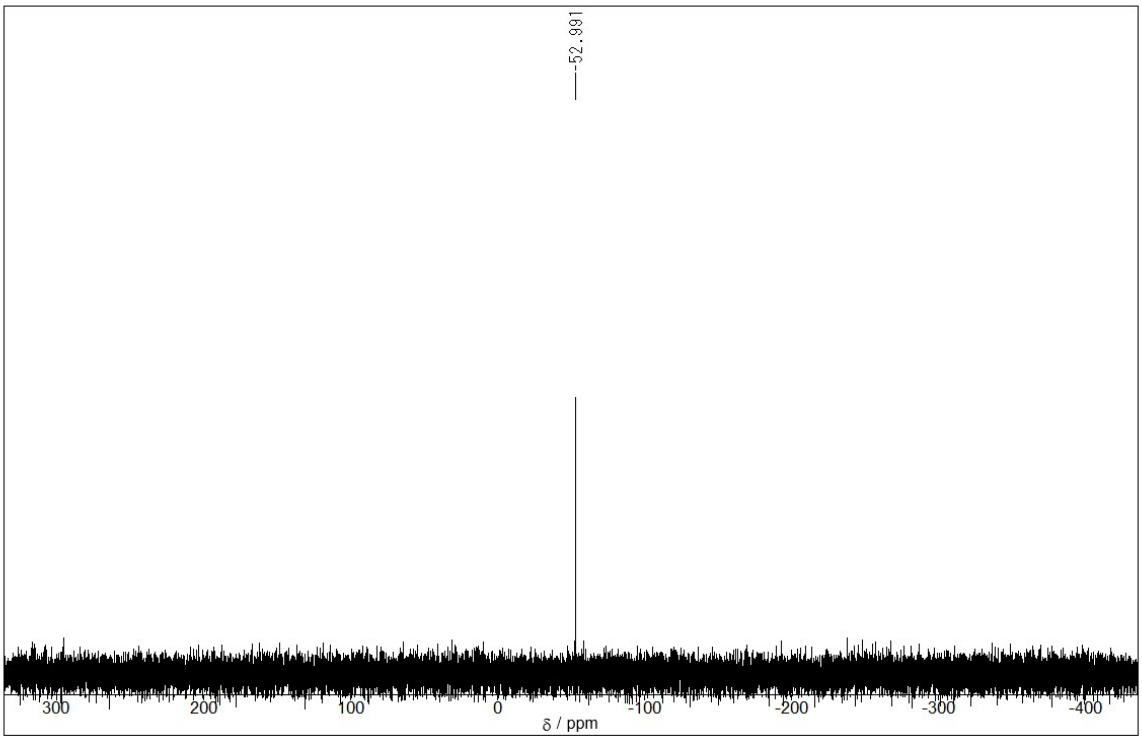

Figure S15. ^{31}P NMR spectrum of **4** (162 MHz, $CDCl_3$)

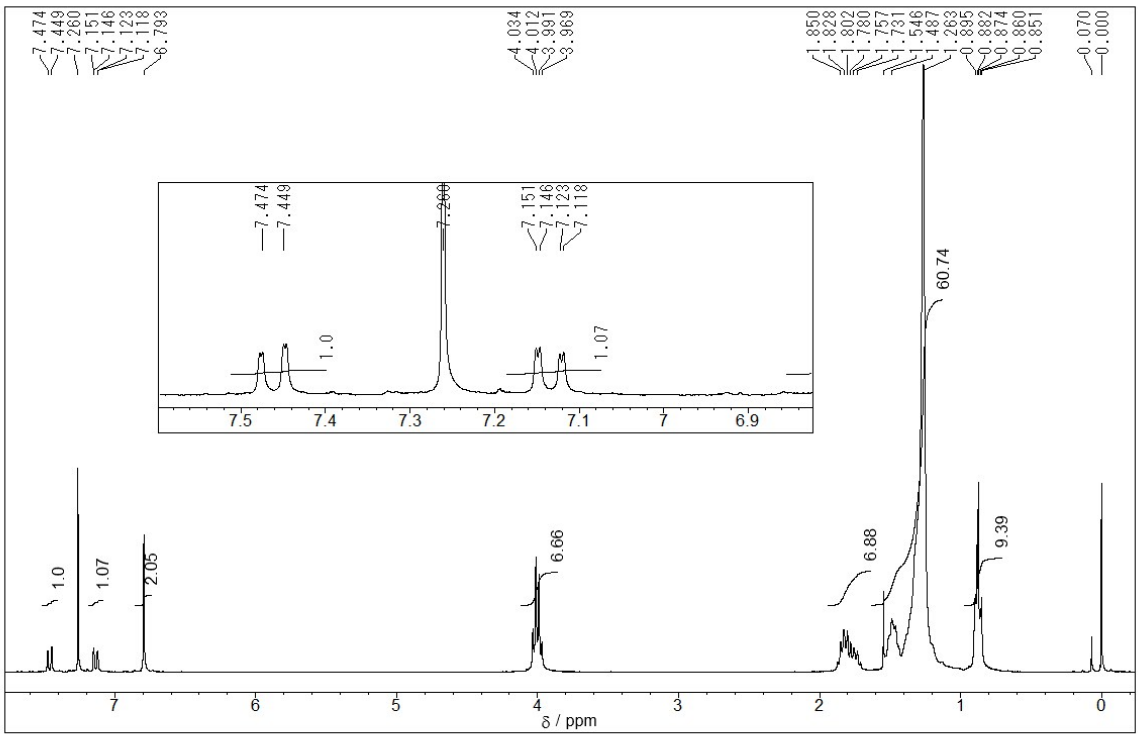

Figure S16. ^{1}H NMR spectrum of **2** (400 MHz, $CDCl_3$)

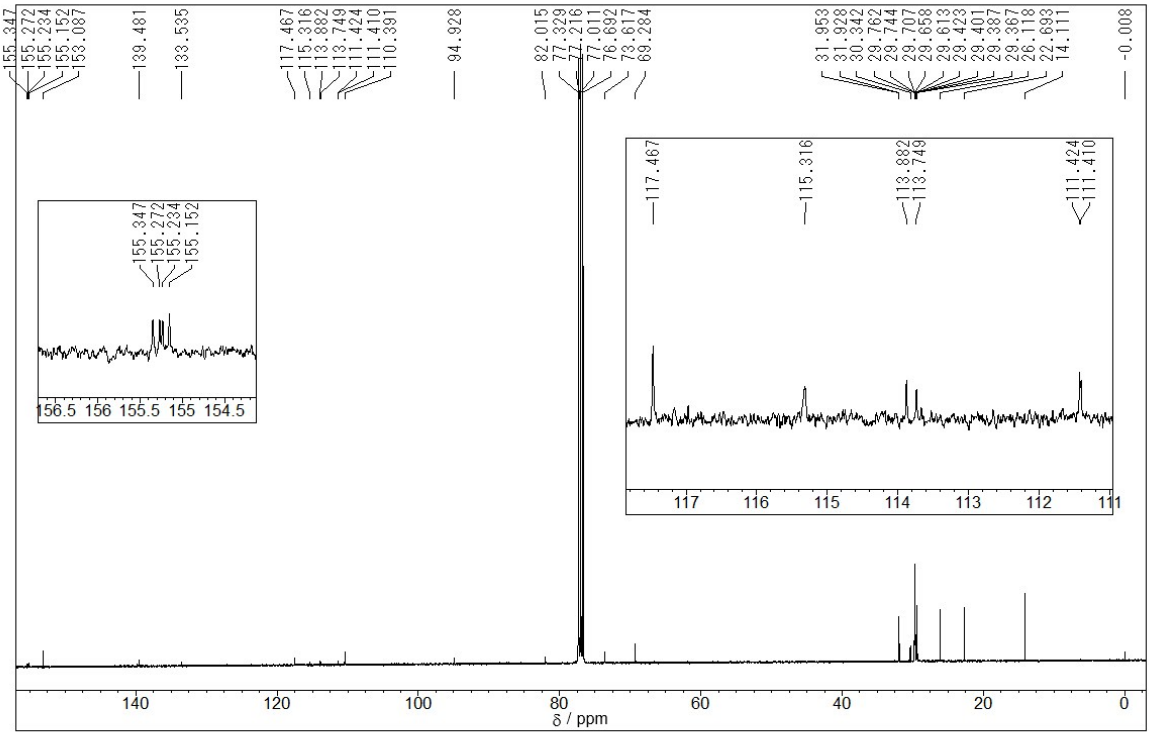

Figure S17. ^{13}C NMR spectrum of **2** (100 MHz, $CDCl_3$)

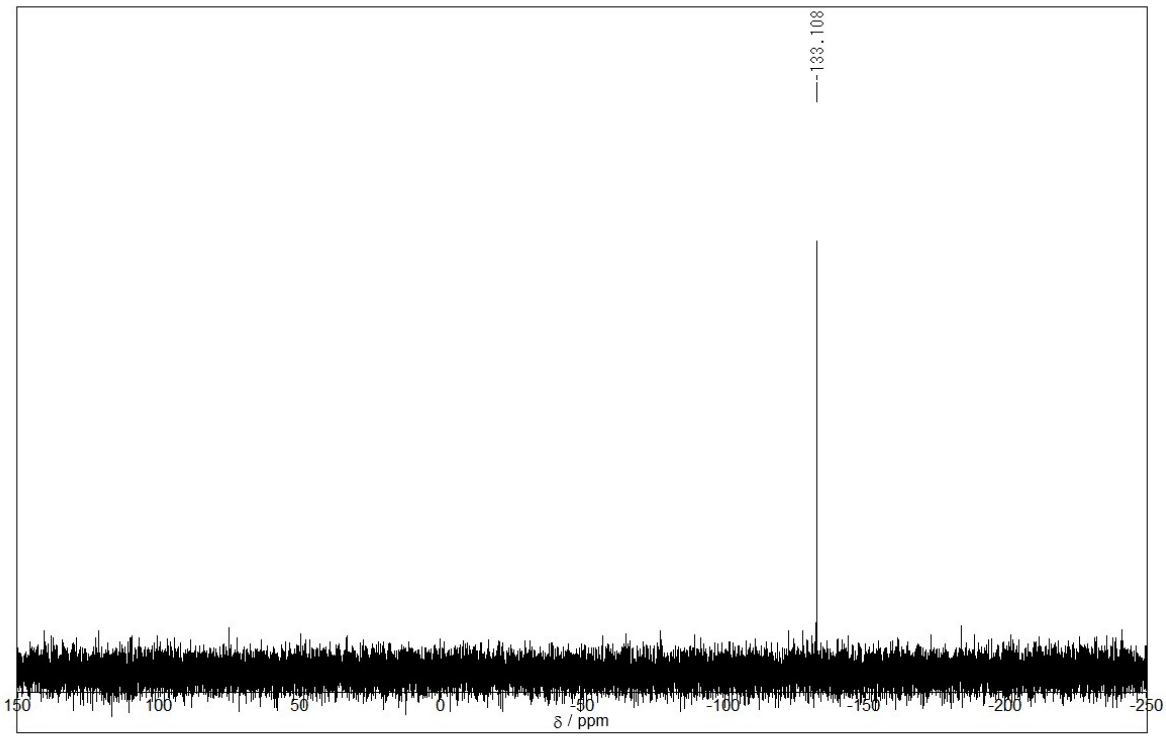

Figure S18. ^{31}P NMR spectrum of **2** (162 MHz, $CDCl_3$)

References

S1 M. Yamamura, T. Saito and T. Nabeshima, *J. Am. Chem. Soc.* **2014**, *136*, 14299.

S2 J. Wu, M. D. Watson, L. Zhang, Z. Wang and K. Müllen, *J. Am. Chem. Soc.* **2004**, *126*, 177.